Int. J. Adv. Eng. Pure Sci. 2026, 38(1): <199-209>
DOI: 10.7240/jeps.1818060

RESEARCH ARTICLE / ARAŞTIRMA MAKALESİ

Picture Fuzzy C-Means–based Ensemble of Forecasting Functions for Financial Time Series Forecasting

Sümeyye POLATER [1], Ufuk YOLCU [2], Furkan KESKİN [2], Özge CAĞCAĞ YOLCU [2]

[1]*Marmara University, Faculty of Science, Department of Statistics, Istanbul, Türkiye*

Abstract

This study introduces a forecasting framework for financial time series that combines multiple forecaster functions built on Picture Fuzzy C-Means (PFCM) clustering. In the proposed framework, the time series is embedded into a lagged-variable space and clustered using Picture Fuzzy C-Means (PFCM), which assigns to each time point three degrees: positive (μ), neutral (η), and negative (ν). For each degree and each cluster, a separate multiple linear regression forecaster is constructed using the corresponding degree, selected nonlinear transformations of that degree, and lagged variables as inputs, while sharing the same target values. Consequently, the procedure produces $3 \times C$ base forecasts that are aggregated in two stages: base forecasts are first combined using the associated degree information and then refined through the neutral/indeterminacy structure to obtain the final forecast. By representing uncertainty through three complementary degrees and enriching the input space with degree-based nonlinear features, the framework captures both linear and nonlinear patterns in a transparent manner. The resulting Picture Fuzzy C-Means–based ensemble of forecasting functions is empirically evaluated on several widely used financial time-series benchmarks and demonstrates competitive forecasting performance.

Keywords: financial time series, picture fuzzy c-means clustering, forecasting functions, bayesian optimization, ensemble learning

I. INTRODUCTION

Time series forecasting models aim to forecast future observations of a variable based on its historical data and has become an essential tool in economics, finance, energy, and environmental sciences. However, real-world time series data often include uncertainty, vagueness, incompleteness, and hesitation caused by noise, human judgments, or measurement errors. These properties may degrade predictive accuracy and reduce interpretability when standard statistical or machine-learning models are applied without an explicit uncertainty representation.

To better represent uncertainty in time-dependent data, fuzzy set theory, introduced by Zadeh [1], provides a mathematical framework for representing uncertainty by assigning each element a degree of membership between 0 and 1. Song and Chissom [2] first defined the fuzzy time series model based on Zadeh's [1] fuzzy set theory to address the shortcomings of classical statistical methods in time series forecasting, introducing the concept of fuzzy time series based on matrix operations. This method was further developed by Chen [3] based on relationship tables. Chen and Chang [4] developed a multivariate fuzzy forecasting model based on fuzzy clustering and fuzzy rule interpolation techniques for multivariate data. Chen and Chen [5] improved forecasting accuracy by combining fuzzy time series and fuzzy variation groups for the TAIEX stock market index forecast. Chen, Chu, and Sheu [6] improved forecasting performance by proposing an automatically weighted multifactor fuzzy time series model for TAIEX forecasting. In addition to the Adaptive Network-Based Fuzzy Inference System (ANFIS) proposed by Jang [7] being used in many studies on time series forecasting problems, Egrioglu et al. [8] developed a new ANFIS (MANFIS) for time series forecasting, increasing its accuracy and learning ability. Sarica et al. [9] combined autoregressive models with the ANFIS framework using a hybrid method called AR–ANFIS, achieving performance improvements in time series forecasting. Turksen [10] developed the concept of fuzzy functions using the least squares (LSE) method, and this approach has opened the door to various studies focusing on the analysis of fuzzy time series. Bas et al. [11] improved the Type-1 fuzzy function approach based on ridge regression, increasing the stability of parameter estimation in time series forecasting and strengthening the generalization ability of the model. Tak [12] introduced a new estimation approach for uncertain data by defining Type-1 probabilistic fuzzy estimation functions. Bas and Egrioglu [13] provided a more effective modelling of uncertainty in complex data sets with the fuzzy regression functions approach based on the Gustafson–Kessel clustering algorithm. Beyond time-series forecasting, fuzzy-set based methods have recently been applied to core operations such as fuzzy set/fuzzy number arithmetic and to regression settings—e.g., by proposing efficient computation of the ridge-type tuning parameter k to enhance fuzzy ridge regression [14][15]. However, classical fuzzy sets

Corresponding Author: UFUK YOLCU, **Tel:** 0216 777 00 00-3326, **E-mail:** ufuk.yolcu@marmara.edu.tr

Submitted: 05.11.2025, **Revised:** 19.12.2025, **Accepted:** 28.01.2026

describe only the membership degree of an element and cannot model hesitation or neutrality. To address this limitation, Atanassov [16] proposed the Intuitionistic Fuzzy Set (IFS), which incorporates both membership and non-membership degrees together with a hesitation degree that reflects the uncertainty between them. Many researchers have further investigated the properties and applications of IFS, particularly in time series forecasting. Cagcag Yolcu et al. [17] presented a new intuitive fuzzy function approach forecasting, enabling a moreflexible representation of uncertainties in the data.

Bas et al. [18] developed the intuitive fuzzy time series function approach to more effectively model uncertainties in time series forecasting and demonstrated that the method provides higher forecast accuracy compared to classical models. Arslan and Cagcag Yolcu [19] proposed a hybrid forecasting model combining intuitive fuzzy time series models with sigma-pi neural networks, achieving effective results in improving accuracy and generalization.

Later, Cuong and Kreinovich [20] extended this concept and introduced the Picture Fuzzy Set (PFS) by adding neutral and refusal degrees, which enables a more comprehensive representation of complex and ambiguous information. Consequently, PFS-based time series models have emerged as a promising direction, improving forecasting accuracy and interpretability by modelling multidimensional uncertainty.

Approaches based on picture fuzzy sets, which allow for more detailed representation of uncertainties in time series forecasting, have become an important research area in recent years. The picture fuzzy time series model, first described by Egrioglu et al. [21], improved forecast accuracy by addressing uncertainty more comprehensively compared to classical and intuitionistic fuzzy time series methods. Extending this fundamental approach, Bas et al. [22] developed a Pi-sigma artificial neural network-based multivariate picture fuzzy time series model for multivariate data, demonstrating the method's effectiveness in multidimensional forecasting problems. Similarly, Rath and Dutta [23] used a revised variant of particle swarm optimization in picture fuzzy time series forecasting to improve the model's convergence rate and forecasting performance. In parallel with these approaches, Thong and Son [24] combined picture fuzzy clustering and rule interpolation methods to provide more accurate modelling of uncertainties in multivariate forecasting problems.

Regardless of the type of fuzzy set they are based on, the first and basic stage of these forecasting models is the stage of producing membership values by fuzzifying the real-valued observed time series. In the literature, depending on the fuzzy set on which it is based, the Fuzzy C-Means Clustering (FCM) algorithm, Intuitionistic Fuzzy C-Means Clustering (I-FCM) algorithm, and Picture Fuzzy C-Means Clustering (P-FCM) algorithm are frequently used for these stage operations. However, the traditional FCM-based models still show limited performance when dealing with nonlinear or noisy data. To overcome this issue, kernel-based extensions, such as the Kernel Fuzzy C-Means (KFCM), have been developed to map data into higher-dimensional spaces for improved cluster separability. In particular, kernelized clustering can improve separability by implicitly mapping observations to a feature space where nonlinear structures are easier to capture. By incorporating these kernel functions into the picture fuzzy framework, the proposed Picture Fuzzy C-Means–based Ensemble of Forecasting Functions (PFCM-b-EFFs) benefits from both enhanced uncertainty representation and improved nonlinear cluster separability, offering a more flexible and powerful clustering approach for complex datasets.

While picture fuzzy clustering improves uncertainty modelling, it does not directly support forecasting. Therefore, in this study, the Type-1 Fuzzy Regression Functions (T1FRFs) component is integrated into the proposed approach as a rule-free fuzzy inference framework. The T1FRFs component enables forecasting by defining fuzzy functional relationships between membership degrees for clusters generated by the (PFCM-b-EFFs). Accordingly, clustering is used to generate informative degrees, and forecasting is performed through regression-based forecaster functions constructed on degree-augmented inputs. Since the T1FRFs, the forecast-generating component of the proposed model, contains a linear regression structure, the input properties of each function may present a problem of collinearity. To address this issue, the structure of the regression function, Ordinary Least Squares (OLS) or Ridge Regression (RR), along with other hyperparameters of the proposed model, is determined over validation sets using Bayesian Optimization (BO). In this way, the model complexity and regularization level are selected in a data-driven manner while preserving a transparent forecasting structure.

In the second section of the study, the proposed methodology is introduced in detail. In the third section, the performance of the proposed model on financial time series is evaluated, and finally, in the last section, the obtained results are discussed.

II. THE PROPOSED METHODOLOGY

Notations

$y_{1:T}$	Univariate time series $\{y_1, \dots, y_T\}$; T total length.
L	Lag length (hyperparameter).
$\boldsymbol{x}_t$	Lag vector at time t: $\boldsymbol{x}_t = [y_{t-1}, \dots, y_{t-L}]^\top \in \mathbb{R}^L$.
n_{tr}, n_{va}, n_{te}	Sizes of train/validation/test with $n_{va} = n_{te}$, $n_{tr} + n_{va} + n_{te} = T$.
$\mathcal{S}(\cdot)$	Columnwise min–max scaler fitted on train features and applied to val/test.
C	Number of clusters in PFCM-b-EFFs (hyperparameter).
m	Picture–fuzzy exponent ($m > 1$; hyperparameter).
α, β, γ	Balance parameters for acceptance, neutrality, rejection in PFCM-b-EFFs (hyperparameters).
$K(\cdot,\cdot)$	Kernel function: RBF (with σ), polynomial (degree d, bias c), or sigmoid (slope a_{sg}, bias c_{sg}).
$\mu_{t,k}, \eta_{t,k}, \nu_{t,k}$	Picture–fuzzy degrees of positive, neutral, negative for sample t in cluster k (each in [0,1]).
π_t	Indeterminacy/Refusal/Hesitation at sample t: $\pi_t = 1 - \sum_{k=1}^{C}(\mu_{t,k} + \eta_{t,k} + \nu_{t,k})$ clipped to [0,1].
$d_{t,k}^{(\delta)}$	Shorthand for $\delta \in \{\mu, \eta, \nu\}$ degree: $d_{t,k}^{(\delta)} \triangleq \delta_{t,k}$.
$Z_k^{(\delta)}$	Degree–augmented design matrix for degree δ and cluster k: columns $\left[\boldsymbol{x}_t,\ d_{t,k}^{(\delta)},\ (d_{t,k}^{(\delta)})^2,\ exp(min\{d_{t,k}^{(\delta)}, 8\}),\ log(d_{t,k}^{(\delta)} + 10^{-6})\right]$.
$w_{t,k}^{(\delta)}$	Sample weight for (δ, k) model: $w_{t,k}^{(\delta)} = (max\{d_{t,k}^{(\delta)}, 0\})^p$ with $p > 0$ (hyperparameter).
$\hat{y}_k^{(\delta)}$	Prediction of the (δ, k) regressor on a given split (val/test).
γ_{in}	Intra–degree fusion sharpness (hyperparameter).
γ_{out}	Inter–degree fusion sharpness (hyperparameter).
$\boldsymbol{\omega}^{(\delta)}$	Intra–degree fusion weights over clusters for degree δ (row–normalized).
$\bar{\pi}_\delta$	Degree–level indeterminacy for δ: average of π_t across clusters (per sample), used in inter–degree fusion.
λ	Ridge regularization coefficient (hyperparameter, $\lambda \geq 0$).
Θ	Hyperparameter set: $\{L, C, m, \alpha, \beta, \gamma,$kernel params$, p, \gamma_{\text{in}}, \gamma_{\text{out}}, \lambda\}$.
$L(\cdot,\cdot)$	Validation metric: RMSE or MSE.
$s_{BO}, s_{\text{PFCM-b-}}$	Fixed random seeds for BO sampling and PFCM-b-EFFs training, respectively.

In this study, a novel forecasting methodology is proposed by integrating kernel-based Picture Fuzzy C-Means clustering with multiple linear regression models optimized through Bayesian search. The procedure is designed to model uncertainty and partial belongingness in financial time-series data by generating four membership degrees— positive(μ), neutral (η), negative (ν), and indeterminacy (π)—for each temporal observation. These membership degrees, together with their nonlinear transformations and lagged inputs, are employed as explanatory variables within locally weighted regression structures. To ensure optimal performance, critical hyperparameters such as the number of clusters, fuzzifier coefficient, kernel type and parameters, and regularization terms are automatically tuned via Bayesian Optimization. This framework allows the simultaneous handling of linear and nonlinear relationships while explicitly representing uncertainty through picture fuzzy memberships, thereby improving the accuracy of time-series forecasting models. The proposed Picture Fuzzy C-Means–based Ensemble of Forecasting Functions (PFCM-b-EFFs) forecast generation process can be given in several basic transactions.

Transaction 1. *Lagged features*. For $t = L + 1, \dots, T$, $\boldsymbol{x}_t = [y_{t-1}, \dots, y_{t-L}]^\top$ and target y_t are built.

Transaction 2. *Splitting data*. The generated lagged features are divided into three sub-data sets: *training*, *validation*, and *test*.

Transaction 3. *Scaling*. Let $(\boldsymbol{X}, \boldsymbol{y})$ denote the feature/target matrices for the selected split. A *min–max* scaler $\mathcal{S}$ is fitted on train columns and applied to val/test to avoid leakage.

Transaction 4. Clustering via Kernel Picture Fuzzy Clustering. On scaled train features $\widetilde{\boldsymbol{X}}_{tr} = \mathcal{S}(\boldsymbol{X}_{tr})$, PFCM-b-EFFs partitions n_{tr} samples into C clusters in a kernel space with parameters $(m, \alpha, \beta, \gamma)$. Each sample obtains picture–fuzzy degrees μ, η, ν, and indeterminacy $\pi = 1 - (\mu + \eta + \nu)$, all clipped to [0,1]. With fixed seed s_{KPFCM}, both the training and subsequent membership inference (for val/test) are deterministic.

Transaction 5. Degree–weighted regressors. For each $\delta \in \{\mu, \eta, \nu\}$ and cluster $k \in \{1, \dots, C\}$ we train two linear models on train: (i) weighted OLS solved via SVD (pinv–safe), (ii) weighted Ridge with parameter λ solved by Cholesky/backslash.

The design is degree–augmented:

$$Z_k^{(\delta)} = \begin{bmatrix} \boldsymbol{x}_t,\ d_{t,k}^{(\delta)},\ (d_{t,k}^{(\delta)})^2,\ exp(min\{d_{t,k}^{(\delta)}, 8\}), \\ log(d_{t,k}^{(\delta)} + 10^{-6}) \end{bmatrix} \quad \textbf{(1)}$$

with weights:

$$w_{t,k}^{(\delta)} = (max\{d_{t,k}^{(\delta)}, 0\})^p,\ p > 0 \quad \textbf{(2)}$$

Transaction 6. Intra–degree fusion (cluster level). Let $\hat{y}_k^{(\delta)}$ be the per–cluster prediction for degree δ. Define the unnormalized weights;

$$\widetilde{\omega}_{t,k}^{(\delta)} = d_{t,k}^{(\delta)} \cdot (1-\pi_t)^{\gamma_{in}} \quad \textbf{(3)}$$

and row–normalize to get $\omega^{(\delta)}$ (uniform fallback when a row sum is zero). The fused degree forecast is

$$\hat{y}^{(\delta)} = \sum_{k=1}^{C} \omega_k^{(\delta)} \hat{y}_k^{(\delta)} \quad \textbf{(4)}$$

Transaction 7. Inter–degree fusion (final output). Compute per–sample degree–level indeterminacies $\bar{\pi}_\mu, \bar{\pi}_\eta, \bar{\pi}_\nu$ (e.g., the mean π_t across clusters). The final forecast is

$$\hat{y} = \frac{(1-\bar{\pi}_\mu)^{\gamma_{out}} \hat{y}^{(\mu)} + (1-\bar{\pi}_\eta)^{\gamma_{out}} \hat{y}^{(\eta)} + (1-\bar{\pi}_\nu)^{\gamma_{out}} \hat{y}^{(\nu)}}{(1-\bar{\pi}_\mu)^{\gamma_{out}} + (1-\bar{\pi}_\eta)^{\gamma_{out}} + (1-\bar{\pi}_\nu)^{\gamma_{out}}} \quad \textbf{(5)}$$

Transaction BO. Bayesian Optimization. We tune Θ over pre–specified ranges using BO with seed s_{BO}. For each trial, we train all models on train and evaluate on validation; the objective is

$$Obj(\Theta) = min\{L(\hat{y}_{OLS}, y_{va}),\ L(\hat{y}_{Ridge}, y_{va})\}, \quad \textbf{(6)}$$

where is RMSE or MSE. The best point is recorded.

Transaction Testing. Final evaluation. With $\Theta^\star$, we rebuild lags with $L^\star$, refit the scaler on train, retrain PFCM-b-EFFs on train (seed $s_{\mathrm{PFCM-b-EFFs}}$), refit all regressors on train, and produce validation/test predictions using Equations (3) and (4). The algorithm for the operation of PFCM-b-EFFs can also be given as pseudo-code as follows.

Briefly, the method first embeds the series into a lagged-input space and uses kernelized picture fuzzy C-means to partition these patterns while quantifying uncertainty via three membership degrees (positive, neutral, and negative). Next, for each cluster and each degree, a simple regression forecaster is trained using the lagged variables together with degree-based features; the resulting base forecasts are then combined by membership-weighted aggregation and refined using the indeterminacy information. Hyperparameters are selected on the validation split, and runtime measurements on the updated datasets are reported to demonstrate practical feasibility.

Algorithm *--- pseudo-code for the proposed PFCM-b-EFFs with Bayesian Hyperparameter Optimization*

Require: Series $y_{1:T}$; test size n_{te}; validation size $n_{\mathrm{va}} = n_{\mathrm{te}}$; search ranges for Θ; seeds $(s_{\mathrm{BO}}, s_{\mathrm{PFCM-b-EFFs}})$; metric $L \in$ {RMSE,MSE}
$n_{\mathrm{tr}} \leftarrow T - n_{\mathrm{va}} - n_{\mathrm{te}}$
Initialize BO with seed s_{BO}; $J^\star \leftarrow +\infty$
for trial = 1, …, N_{BO} do
    Sample $\Theta = \{L, C, m, \alpha, \beta, \gamma, \text{kernel params}, p, \gamma_{\mathrm{in}}, \gamma_{\mathrm{out}}, \lambda\}$
    Build lags with L; split into train/validation
    Fit min–max scaler on train; transform train/validation
    Train PFCM-b-EFFs on train with seed $s_{\mathrm{PFCM-b-EFFs}}$; infer (μ, η, ν, π) on train/validation
    for $\delta \in \{\mu, \eta, \nu\}$ do
        for $k = 1$ to C do
            Form $Z_k^{(\delta)}$ (Eq. (1)); set weights $w_{t,k}^{(\delta)}$
            Fit weighted OLS and weighted Ridge(λ) on train
            Predict $\hat{y}_k^{(\delta)}$ on validation
        end for
        Intra–degree fusion (Eq. (3)) to get $\hat{y}^{(\delta)}$
    end for
    Inter–degree fusion (Eq. (4)) to get $(\hat{y}_{\mathrm{OLS}}, \hat{y}_{\mathrm{Ridge}})$
    $J \leftarrow \min\left(L(\hat{y}_{\mathrm{OLS}}, y_{\mathrm{va}}),\ L(\hat{y}_{\mathrm{Ridge}}, y_{\mathrm{va}})\right)$
    if $J < J^\star$ then
        $J^\star \leftarrow J$; $\Theta^\star \leftarrow \Theta$
    end if
end for
Final: Rebuild with $L^\star$; refit scaler on train; train PFCM-b-EFFs on train (seed $s_{\mathrm{PFCM-b-EFFs}}$)
Refit all (δ, k) OLS/Ridge on train; predict on validation/test; apply the same fusions
Return final validation/test metrics; model artifacts; seeds $(s_{\mathrm{BO}}, s_{\mathrm{PFCM-b-EFFs}})$

III. APPLICATIONS

In this empirical study, eleven daily equity indices are considered. These are the TAIEX—Taiwan Stock Exchange Capitalization Weighted Index—observed from 1999 to 2004 and from 2021 to 2025. For each year, the observations within that calendar year are treated as a separate forecasting task. Each series is divided into training, validation, and test sets, with the validation and test sets of equal size, while the remaining observations are used for training. All models are tuned on the validation set and evaluated out-of-sample on the test set using a one-step-ahead forecasting protocol. Implementation details, including the sizes of the training, validation, and test sets, are summarized in Table 1.

Table 1. Time series and basic properties of analysis

Id	Name	Year	# observation	# train set	# validation & test set
1		1999	266	176	45
2		2000	271	177	47
3	TAIEX	2001	244	158	43
4		2002	248	162	43
5		2003	249	162	43
6		2004	250	160	45
7		2021	244	156	44
8		2022	246	158	44
9		2023	239	153	43
10		2024	242	156	43
11		2025	232	170	31

The forecasting framework is tuned with Bayesian Optimization (BO) over a joint space that includes the lag length and the hyperparameters of Picture Fuzzy C-Means–based Ensemble of Forecasting Functions (PFCM-b-EFFs), the regression stage, and the intra-/inter-degree combination exponents. BO is run with a deterministic objective—the validation error—and the expected-improvement-plus acquisition. Each BO run uses 60 objective evaluations, and fixed random seeds for reproducibility (separate seeds for BO sampling and PFCM-b-EFFs initialization).*Objective*: For a candidate hyperparameter vector θ, PFCM-b-EFFs is trained only on the training split, the memberships on the validation split are computed, both weighted *OLS* and weighted *Ridge* regressions (weights derived from degrees) are fitted, validation predictions are produced, and the scalar objective $min\{RMSE\ OLS,\ RMSE\ Ridge\}$ is taken. *Data protocol*: For each year/series, the data are partitioned into train/validation/test with equal-sized validation and test sets; the remaining samples are used for training. Feature scaling (min–max) is fit on training lags only and applied to validation/test. PFCM-b-EFFs is never refit on validation or test during BO. *Search space*: The following variables are optimized jointly:

- *Lag length*: $L \in [L_{min} = 2, L_{max} = 20] \cap \mathbb{Z}$
- # clusters: $C \in [2, 8] \cap \mathbb{Z}$
- Fuzzifier / Fuzziness index: $m \in [1.3, 3.0]$
- Trade-offs: $\alpha, \beta, \gamma \in [0.5, 2.0]$
- Degree exponent: $p \in [0.3, 3.0]$ (weights are $w = max(d, 0)^p$
- Intra-degree combination: $\gamma_{in} \in [0.3, 3.0]$ (sharpens cluster-level weights)
- Inter-degree combination: $\gamma_{out} \in [0.3, 3.0]$ (controls $\mu - \eta - \nu$ fusion)
- Ridge regularization: $\lambda \in [10^{-5}, 10^{2}]$ with **log transform** (searches exponentially)
- Kernel choice: $\{rbf, poly, sg\}$:
  - For rbf - Gaussian kernel – bandwidth $\sigma \in [0.05, 5.00]$

$$\mathrm{k}_{\mathrm{rbf}}(\mathbf{x}, \mathbf{z}) = \exp\left(-\frac{\|\mathbf{x}-\mathbf{z}\|^2}{2\sigma^2}\right) = \exp(-\gamma\|\mathbf{x}-\mathbf{z}\|^2); \quad \gamma = \frac{1}{2\sigma^2} \tag{7}$$

  - For $poly$ - Polynomial kernel – degree $d \in [2, 5] \cap \mathbb{Z}$; bias $c_{poly} \in [2, 5]$

$$k_{poly}(\boldsymbol{x}, \boldsymbol{z}) = (\boldsymbol{x}^T\boldsymbol{z} + c)^d \ \boldsymbol{or}\ k_{poly}(\boldsymbol{x}, \boldsymbol{z}) = (\alpha\boldsymbol{x}^T\boldsymbol{z} + c)^d; \quad d \geq 1 \in \mathbb{N}; c \geq 0;\ \alpha > 0 \tag{8}$$

  - For sg- Sigmoid kernel – degree $\alpha_{sg} \in [0.1, 5.0] \cap \mathbb{Z}$; bias $c_{sg} \in [-3, 3]$

$$k_{\,sigmoid}(\boldsymbol{x}, \boldsymbol{z}) = tanh(\alpha\boldsymbol{x}^T\boldsymbol{z} + c); \quad d \geq 1 \in \mathbb{N}; c \geq 0;\ \alpha > 0 \tag{9}$$

The forecast performance of the proposed *PFCM-b-EFFs* is evaluated with twelve methods on six daily TAIEX series —denoted T99–T04—using rolling train/validation/test splits (validation and test widths are specified for each year). Forecast accuracy is reported as RMSE, and for each time series, methods are ranked from best (Rank = 1) to worst based on their RMSE in that series. The average RMSE and the average Rank across T99–T04 summarize the overall performance. All results are presented in Table 2.

The proposed *PFCM-b-EFFs* achieves the best overall accuracy and the most favourable ranking profile. It has the lowest average $RMSE = 65$ with $Average\ Rank = 1.14$, placing first on five of the six series (*T99*, *T00*, *T01*, *T03*, *T04*) and second on the remaining one (*T02*). On a per-series basis, *PFCM-b-EFFs* delivers RMSEs of 95, 100, 103, 61, 47, 48 for *T99–T04*, respectively. The closest competitor is model [25] (*Average RMSE* 67, *Average Rank* 2.14), followed by [10] (69, 4.00) and MANFIS [8] (70, 6.00). Classical neuro-fuzzy baselines lag behind: ANFIS [7] averages 75 *RMSE* (9.57), while [3] is the weakest with 102 *RMSE* (12.29).
The PFCM-b-EFFs design—cluster-wise linear models driven by picture-fuzzy degrees and their nonlinear

transforms, followed by degree-level aggregation—delivers both accuracy gains across all six TAIEX series, offering a new state-of-the-art model within this comparison.

Table 2. RMSE-based performance ranking of competing models on TAIEX (T99-T04) datasets.

Models	Value& Rank	Time Series						Average
		T99	T00	T01	T02	T03	T04	
[3]	V	120	176	148	101	74	84	102
	R	10	11	13	13	13	13	13
	Avrg. R.	12.29						
[4]	V	102	129	113	67	54	60	74
	R	7	9	7	10	10	11	10
	Avrg. R.	9.14						
[5]	V	112	124	115	71	58	58	76
	R	9	7	11	12	12	10	12
	Avrg. R.	10.43						
[6]	V	100	120	114	67	52	52	71
	R	5	4	10	10	5	4	7
	Avrg. R.	6.43						
ANFIS [7]	V	101	137	115	66	57	61	75
	R	6	10	11	6	11	12	11
	Avrg. R.	9.57						
MANFIS [8]	V	102	125	112	63	52	54	70
	R	7	8	6	3	5	7	6
	Avrg. R.	6.00						
AR-ANFIS [9]	V	98	123	111	66	52	54	71
	R	2	6	5	6	5	7	7
	Avrg. R.	5.43						
[10]	V	99	120	113	63	49	52	69
	R	4	4	7	3	2	4	4
	Avrg. R.	4.00						
[25]	V	98	113	109	**60**	49	49	67
	R	2	2	4	**1**	2	2	2
	Avrg. R.	2.14						
[12]	V	---	---	113	66	53	54	72
	R			7	6	8	7	9
	Avrg. R.	7.40						
[26]	V	---	119	104	64	51	52	68
	R		3	2	5	4	4	3
	Avrg. R.	3.50						
[13]	V	---	---	106	66	53	51	69
	R			3	6	8	3	4
	Avrg. R.	4.80						
PFCM-b-EFFs	V	**95**	**100**	**103**	61	**47**	**48**	**65**
	R	**1**	**1**	**1**	2	**1**	**1**	**1**
	Avrg. R.	**1.14**						

To reinforce the RMSE-based comparison, the individual forecasting accuracy of the proposed PFCM-b-EFFs model was further evaluated using the Mean Absolute Percentage Error (MAPE). Unlike scale-dependent metrics such as RMSE or MAE, MAPE expresses the forecasting error as a percentage of the observed value, enabling an individual evaluation of the forecasting methods. Table 3 summarizes the MAPE values (%) of the proposed model for each TAIEX time series (T99–T04). The average MAPE across all series is also reported to quantify the model's overall proportional accuracy.

Table 3. MAPE (%) results of the PFCM-b-EFFs on TAIEX datasets.

Time Series						Average
T99	**T00**	**T01**	**T02**	**T03**	**T04**	
0.99	1.44	1.65	1.03	0.66	0.60	1.06

The MAPE results indicate that the PFCM-b-EFFs model maintains exceptionally low proportional forecasting errors across all TAIEX datasets. The average MAPE of 1.06% demonstrates that, on average, the model's forecasts deviate from the actual values by roughly one percent, underscoring both its accuracy and stability. The lowest errors are observed for T03 (0.66%) and T04 (0.60%), corresponding to later periods when the model exhibits enhanced adaptivity to smoother index dynamics. Even for the more volatile years (T00–T01), the MAPE values remain below 1.7%, confirming the strong generalization ability of the PFCM-b-EFFs across varying temporal structures. These findings validate that the proposed fuzzy–regression hybrid framework not only achieves superior RMSE performance but also sustains high proportional precision, making it a reliable and effective forecasting model for financial time-series applications.

To further examine the validity and fidelity of the proposed PFCM-b-EFFs model, an additional regression-based consistency test was conducted between the forecasted ($\hat{Y}_t$) and actual (Y_t) values of each TAIEX time series. This relationship was evaluated through a simple linear regression model formulated as:

$$Y_t = \beta \hat{Y}_t + \varepsilon_t \quad , t = 1,2, \cdots, n_{te} \tag{10}$$

In this framework, β represents the *regression coefficient* describing the proportional relationship between the forecasts and true observations, while R^2 quantifies the *goodness of fit*. Ideally, a *perfectly accurate model* should yield both coefficients close to 1 ($\beta \approx 1$, $R^2 \approx 1$), implying that the model's forecasts align almost exactly with actual outcomes. Furthermore, when the 95% *confidence interval* of β includes 1, it indicates that the null hypothesis of perfect agreement cannot be rejected at the 5% significance level—demonstrating *statistical consistency* between predicted and observed series.

Table 4. Regression-based validity analysis between actual and forecasted TAIEX values.

Time Series	$Y = \widehat{\beta} Y_{forecast}$	**95% Confidence Interval of β**		R^2 **(%)**
		Lower Bound	**Upper Bound**	
T99	$Y = 1.002784 Y_{forecast}$	0.999164	1.006405	99. 9858
T00	$Y = 1.001525 Y_{forecast}$	0.995963	1.007087	99. 9650
T01	$Y = 1.000458 Y_{forecast}$	0.993742	1.007175	99. 9535
T02	$Y = 0.999333 Y_{forecast}$	0.995249	1.003418	99. 9828
T03	$Y = 1.000316 Y_{forecast}$	0.997796	1.002837	99. 9935
T04	$Y = 0.999767 Y_{forecast}$	0.997277	1.002258	99. 9932

The regression-based validation confirms the remarkable accuracy and statistical reliability of the PFCM-b-EFFs forecasts. Across all six TAIEX datasets, the estimated β coefficients remain extremely close to 1, varying within the narrow range of $0.999 - 1.003$, and all corresponding 95% confidence intervals encompass 1. This indicates a strong proportional equivalence between forecasted and actual values, affirming that the model neither systematically underestimates nor overestimates the target series. Moreover, the R^2 values consistently exceed 99.95%, suggesting that over 99.9% of the variation in the actual series is captured by the predicted values. Such near-perfect explanatory power highlights the robust linear alignment between predictions and true observations, further evidencing that the model's internal structure—built on picture-fuzzy clustering and multi-degree regression fusion—achieves an almost one-to-one correspondence with reality.

To further illustrate the alignment between predicted and actual values, scatter plots were generated for each TAIEX time series, where the horizontal axis represents the model forecasts and the vertical axis denotes the observed values (Figure 1). Each plot also includes the fitted regression line (in red), reflecting the degree of linear correspondence between the two. The

scatter plots reveal an almost perfect linear relationship between the forecasts and actual observations across all six TAIEX datasets. The points cluster closely around the fitted regression line, confirming that the predicted values closely follow the real market dynamics with minimal dispersion. No significant systematic bias or heteroscedastic pattern is observed, further reinforcing the consistency of the model's performance. These graphical findings complement the earlier statistical validation (Table 4), demonstrating that the PFCM-b-EFFs model provides highly stable, unbiased, and reliable forecasts for financial time series forecasting.

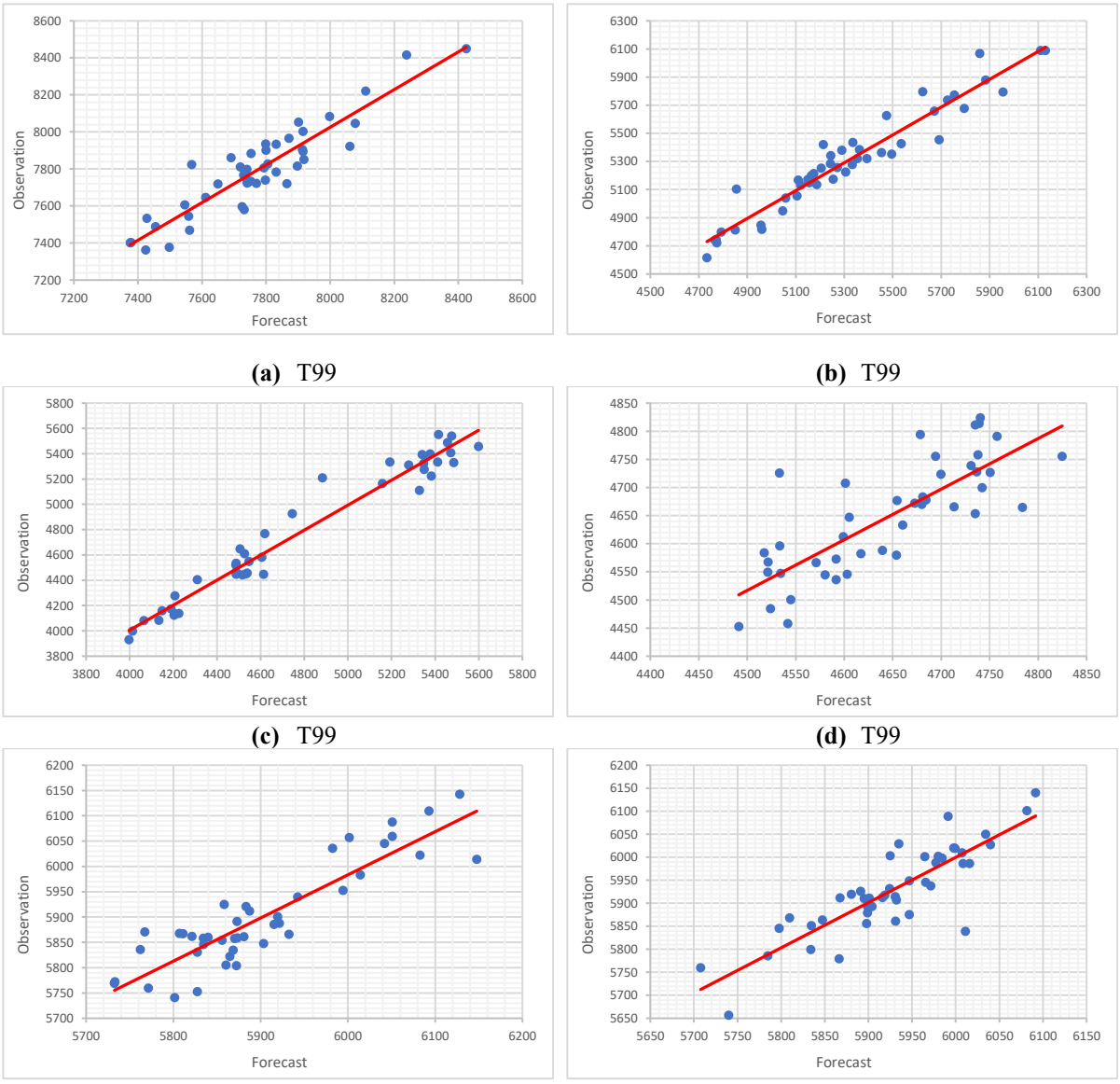

Figure 1. Scatter plots of actual vs. forecasted values for TAIEX series with fitted regression lines

Moreover, the applications were extended by incorporating five newly collected daily TAIEX price series spanning 2021–2025 to examine the proposed methodology under more recent market conditions. These datasets were processed using the same experimental protocol, and the forecasting performance was re-assessed to provide a stronger basis for interpretation. For a more comprehensive evaluation, the proposed model was benchmarked against six baseline methods, namely *Fuzzy Regression Functions* (FRFs), *Intuitionistic Fuzzy Regression Functions* (IFRFs), *Random Forest* (RF), *Gradient Boosting* (GB), *Multi-Layer Perceptron* (MLP), and Long Short-Term Memory (LSTM). The comparative results, reported in terms of RMSE, are summarized in Table 5, which provides a consolidated view of the relative accuracy of all competing approaches on the updated TAIEX series. In addition to accuracy, Table 5 reports the elapsed time (seconds) for the proposed method on each series, indicating that its computational cost remains moderate and stable across T21–T25 (approximately 17–28 s).

Table 5. RMSE comparison of forecasting models across five TAIEX (T21-T25)

Models	Time Series				
	T21	**T22**	**T23**	**T24**	**T25**
GB	126.01	409.18	364.26	311.26	2175.13
RF	153.67	494.85	297.28	275.78	2495.02
MLP	216.59	451.37	166.13	364.71	535.72
LSTM	121.87	183.11	133.7	263.83	448.29
FFRs	126.02	169.13	132.85	262.08	395.53
IFFRs	125.72	169.38	130.87	261.94	369.13
PFCM-b-EFFs	**104.96**	**146.82**	**96.18**	**204.01**	**336.76**
Elapsed time (sec.)	17.18	26.58	27.93	17.88	25.41
Progress (%)	**13.88**	**13.19**	**26.51**	**22.12**	**8.77**

Table 6. One-Sided Diebold–Mariano test results for the PFCM-b-EFFs versus baseline models (T21–T25)

Baseline Models	Test Results	T21	T22	T23	T24	T25
FFRs	DM	2.0449	1.8573	5.1844	4.0818	1.863
	p (one-sided)	0.0204	0.0351	<0.0001	<0.0001	0.0312
IFFRs	DM	2.088	1.8582	5.1262	4.068	1.4879
	p (one-sided)	0.0184	0.035	<0.0001	<0.0001	0.0684
GB	DM	2.2027	2.7102	5.0973	3.4574	12.0366
	p (one-sided)	0.0138	0.0048	<0.0001	<0.0001	<0.0001
RF	DM	1.9478	2.8795	4.1836	2.3104	13.7133
	p (one-sided)	0.0257	0.0031	<0.0001	0.0104	<0.0001
MLP	DM	2.9547	4.3977	3.9389	3.0735	2.8437
	p (one-sided)	0.0016	<0.0001	<0.0001	0.0011	0.0022
LSTM	DM	1.9941	1.8493	3.2724	2.7584	2.2781
	p (one-sided)	0.0231	<0.0001	<0.0001	0.0029	0.0114

Table 5 summarizes the RMSE results across five time series and shows that the proposed PFCM-b-EFFs consistently attains the lowest RMSE, outperforming all baseline models in every case. The Progress (%) row further indicates that, relative to the best-performing baseline, the proposed method improves forecast accuracy by 8.77% to 26.51% across the series.

To rigorously validate that the observed RMSE reductions reflect a genuine improvement in predictive accuracy—rather than sampling variability—we conducted one-sided Diebold–Mariano tests to formally compare the proposed model's out-of-sample squared-error losses against each baseline under the directional hypothesis of superior performance (see Table 6). Across the T21–T25 test sets, the one-sided Diebold–Mariano (DM) tests whether the proposed model achieves lower expected squared forecast error than each competing method consistently support the superiority of the proposed approach. In line with the RMSE rankings, the one-sided DM evidence indicates that the proposed model yields statistically significant accuracy gains against the principal machine-learning baselines, including tree-based ensembles (GB and RF) and neural-network predictors (MLP and LSTM), with the strongest and most stable improvements observed in these comparisons. Relative to the closest competitors (FRFs and IFRFs), the one-sided results remain largely favorable, although the strength of evidence varies across datasets, reflecting narrower performance gaps and thus more modest effect sizes in the tightest match-ups. Overall, the one-sided DM findings, together with the error-level summaries, indicate that the proposed method delivers a robust and reproducible improvement in forecast accuracy across all examined datasets, with particularly pronounced gains over standard machine-learning benchmarks and generally positive advantages over the most competitive fuzzy/regression-based alternatives.

IV. RESULTS AND DISCUSSION

The empirical findings obtained from the TAIEX datasets clearly demonstrate the forecasting efficiency and generalization ability of the proposed PFCM-b-EFFs model. Through a combination of kernel picture fuzzy clustering and multi-degree regression fusion, the model effectively captures both linear and nonlinear dependencies in financial time series data while maintaining strong approaching against uncertainty and indeterminacy.

Financial index levels such as TAIEX typically exhibit strong persistence, implying that successive observations are highly correlated and that simple lag-based baselines can already be competitive. In such settings, very high goodness-of-fit measures (e.g., R^2) and low relative errors (e.g., MAPE) are not unusual when models are evaluated in a one-step-ahead, strictly out-of-sample framework. For this reason, hyperparameters are tuned using only the validation split, while the test split is reserved solely for final reporting. The proposed method is designed to leverage this persistence through lagged inputs while modelling uncertainty via picture-fuzzy membership degrees.

For the TAIEX datasets (1999–2004), the comparative performance analysis (Table 2) revealed that the *PFCM-b-EFFs* model consistently outperformed all competing models across nearly all benchmark years. The proposed approach achieved the lowest RMSE values and the best average ranking (1.14) among thirteen competing models, confirming its superior accuracy and stability in forecasting stock index movements.

Complementary to RMSE-based evaluations, the MAPE analysis provided in Table 3 further validates the model's high consistency. The results indicated that forecast errors remained below 2% on average for all TAIEX series. This finding highlights the model's scale-independent accuracy and its strong suitability for heterogeneous financial environments.

To verify the internal consistency between forecasts and real observations, a regression-based validity analysis was conducted (Table 4). The results showed regression coefficients (β) remarkably close to 1, with 95% confidence intervals including unity, and R^2 values exceeding 99.9%. These outcomes indicate an almost perfect linear correspondence between forecasted and actual values. Furthermore, the accompanying scatter plots (Figure 3) visually support this conclusion: the predicted and observed values align closely along the identity line for all series, demonstrating a highly stable forecast structure.

The additional experiments on the updated TAIEX datasets (T21–T25) confirm that the proposed KPFCM-based framework preserves its forecasting advantage over the baseline methods (FRFs, IFRFs, ETS, ARIMA, Random Forest, Gradient Boosting, MLP, and LSTM), with the comparative results reported in Table 5.

Overall, the proposed *PFCM-b-EFFs* model exhibits strong forecasting power, and statistical reliability across all evaluation metrics. These results suggest that the *PFCM-b-EFFs* framework can serve as a reliable and interpretable alternative for complex financial time series forecasting tasks, outperforming existing neuro-fuzzy and regression-based hybrid models.

ACKNOWLEDGMENT

This study was supported by Marmara University Scientific Research Projects Committee (BAPKO) under the Master's Thesis Project, Project No: FYL-2025-11872.

REFERENCES

[1] Zadeh, L.A. (1965). Fuzzy sets. Information and control. 8(3), 338–353.

[2] Song, Q. and Chissom, B.S. (1993). Forecasting enrollments with fuzzy time series—Part I. Fuzzy sets and systems. 54(1), 1–9.

[3] Chen, S.-M. (1996). Forecasting enrollments based on fuzzy time series. Fuzzy sets and systems. 81(3), 311–319.

[4] Chen, S.-M. and Chang, Y.-C. (2010). Multi-variable fuzzy forecasting based on fuzzy clustering and fuzzy rule interpolation techniques. Information sciences. 180(24), 4772–4783.

[5] Chen, S.-M. and Chen, C.-D. (2010). TAIEX forecasting based on fuzzy time series and fuzzy variation groups. IEEE Transactions on Fuzzy Systems. 19(1), 1–12.

[6] Chen, S.-M., Chu, H.-P., and Sheu, T.-W. (2012). TAIEX forecasting using fuzzy time series and automatically generated weights of multiple factors. IEEE Transactions on Systems, Man, and Cybernetics-Part A: Systems and Humans. 42(6), 1485–1495.

[7] Jang, J.-S. (1993). ANFIS: adaptive-network-based fuzzy inference system. IEEE transactions on systems, man, and cybernetics. 23(3), 665–685.

[8] Egrioglu, E., et al. (2014). A new adaptive network based fuzzy inference system for time series forecasting. Aloy J Soft Comput Appl. 2(1), 25–32.

[9] Sarıca, B., Eğrioğlu, E., and Aşıkgil, B. (2018). A new hybrid method for time series forecasting: AR–ANFIS. Neural Computing and Applications. 29(3), 749–760.

[10] Türkşen, I.B. (2008). Fuzzy functions with LSE. Applied Soft Computing. 8(3), 1178–1188.

[11] Bas, E., et al. (2019). Type 1 fuzzy function approach based on ridge regression for forecasting. Granular Computing. 4(4), 629–637.

[12] Tak, N. (2020). Type-1 possibilistic fuzzy forecasting functions. Journal of Computational and Applied Mathematics. 370, 112653.

[13] Bas, E. and Egrioglu, E. (2022). A fuzzy regression functions approach based on Gustafson-Kessel clustering algorithm. Information Sciences. 592, 206–214.

[14] Homaida, A., Pekalp, M. H., & Ebegil, M. (2024). Bulanık Küme ve Bulanık Sayı: Uygulamalarla Aritmetik İşlemler. Dicle Üniversitesi Fen Bilimleri Enstitüsü Dergisi, 13(2), 223-247.

[15] Homaida, A., Pekalp, M. H., & Ebegil, M. (2025). Efficient k Value Computation for Enhanced Fuzzy Ridge Regression. Journal of Computational and Applied Mathematics, 116813.

[16] Atanassov, K.T. (1999). Intuitionistic fuzzy sets, in Intuitionistic fuzzy sets: theory and applications, Springer. p. 1–137.

[17] Cagcag Yolcu, O., et al. (2020). A new intuitionistic fuzzy functions approach based on hesitation margin for time-series prediction. Soft Computing-A Fusion of Foundations, Methodologies & Applications. 24(11).

[18] Bas, E., Yolcu, U., and Egrioglu, E. (2021). Intuitionistic fuzzy time series functions approach for time series forecasting. Granular computing. 6(3), 619–629.

[19] Arslan, S.N. and Cagcag Yolcu, O. (2022). A hybrid sigma-pi neural network for combined intuitionistic fuzzy time series prediction model. Neural Computing and Applications. 34(15), 12895–12917.

[20] Cuong, B.C. and Kreinovich, V. (2013). Picture fuzzy sets-a new concept for computational intelligence problems. in 2013 third world congress on information and communication technologies (WICT 2013). IEEE.

[21] Egrioglu, E., et al. (2020). Picture fuzzy time series: Defining, modeling and creating a new forecasting method. Engineering Applications of Artificial Intelligence. 88, 103367.

[22] Bas, E., Egrioglu, E., and Tunc, T. (2023). Multivariate picture fuzzy time series: New definitions and a new forecasting method based on Pi-sigma artificial neural network. Computational Economics. 61(1), 139–164.

[23] Rath, S. and Dutta, D. (2024). Picture Fuzzy Time Series Forecasting with a Novel Variant of Particle Swarm Optimization. SN Computer Science. 5(1), 193.

[24] Thong, P.H. and Son, L.H. (2015). A new approach to multi-variable fuzzy forecasting using picture fuzzy clustering and picture fuzzy rule interpolation method. in Knowledge and Systems Engineering: Proceedings of the Sixth International Conference KSE 2014. Springer.

[25] Bas, E., Yolcu, U., and Egrioglu, E. (2020). Picture fuzzy regression functions approach for financial time series based on ridge regression and genetic algorithm. Journal of Computational and Applied Mathematics. 370, 112656.

[26] Tak, N. and İnan, D. (2022). Type-1 fuzzy forecasting functions with elastic net regularization. Expert Systems with Applications. 199, 116916.